City Research Online

City St George's, University of London

Citation: Rane, S., Kovacevic, A., Stosic, N. & Kethidi, M. (2013). Grid deformation strategies for CFD analysis of screw compressors. International Journal of Refrigeration, 36(7), pp. 1883-1893. doi: 10.1016/j.ijrefrig.2013.04.008

This is the accepted version of the paper.

This version of the publication may differ from the final published version. To cite this item please consult the publisher's version.

Permanent repository link: https://openaccess.city.ac.uk/id/eprint/12667/

Link to published version: https://doi.org/10.1016/j.ijrefrig.2013.04.008

Copyright and Reuse: Copyright and Moral Rights remain with the author(s) and/or copyright holders. Copies of full items can be used for personal research or study, educational, or not-for-profit purposes without prior permission or charge, unless otherwise indicated, provided that the authors, title and full bibliographic details are credited, a hyperlink and/or URL is given for the original metadata page and the content is not changed in any way. For full details of reuse please refer to City Research Online policy.

City Research Online: http://openaccess.city.ac.uk/ publications@citystgeorges.ac.uk

Elsevier Editorial System(tm) for International Journal of Refrigeration
Manuscript Draft

Manuscript Number: JIJR-D-12-00417R2

Title: Grid Deformation Strategies for CFD Analysis of Screw Compressors

Article Type: Special Issue: Compressor Technology

Keywords: Twin Screw Compressor; CFD; Space Conservation; Deforming grids; Key-Frame Re-meshing; User Defined Nodal Displacement.

Corresponding Author: Mr. Sham Ramchandra Rane, Ph.D.

Corresponding Author's Institution: City University London

First Author: Sham Ramchandra Rane, Ph.D.

Order of Authors: Sham Ramchandra Rane, Ph.D.; Ahmed Kovacevic, Dipl Ing, MSc, PhD, CEng, FIMechE; Nikola Stosic, Dipl Ing (Mech), MSc(Eng), Dr(Sci); Madhulika Kethidi, PhD

Abstract: Customized grid generation of twin screw machines for CFD analysis is widely used by the refrigeration and air-conditioning industry today, but is currently not suitable for topologies such as those of single screw, variable pitch or tri screw rotors. This paper investigates a technique called key-frame re-meshing that supplies pre-generated unstructured grids to the CFD solver at different time steps. To evaluate its accuracy, the results of an isentropic compression-expansion process in a reciprocating piston cylinder arrangement have been compared. Three strategies of grid deformation; diffusion equation mesh smoothing, user defined nodal displacement and key-frame remeshing have been assessed. There are many limitations to key-frame re-meshing. It requires time consuming pre-processing, has limited applicability to complex meshes and leads to inaccuracies in conservation of calculated variables. It was concluded that customized tools for generation of CFD grids are required for complex screw machines.

Response to Reviewers: Response to Reviewer comments is in file JIJR-D-12-00417-Review.doc

Grid Deformation Strategies for CFD Analysis of Screw Compressors

Sham Rane*, Ahmed Kovacevic, Nikola Stosic, Madhulika Kethidi

Highlights:

- Key-Frame Grid Re-meshing investigated for Screw compressor CFD modeling.
- Accuracy of calculation evaluated through analysis of an isentropic process in a Piston-Cylinder.
- Successful use of customized grid generator demonstrated for twin screw compressor CFD analysis.
- The need for development of customized grid generators for multi-rotor screw machines highlighted.

IJR_Sham_2012_CheckList.docx
Click here to view linked References

Grid Deformation Strategies for CFD Analysis of Screw Compressors

Sham Rane*, Ahmed Kovacevic, Nikola Stosic, Madhulika Kethidi

One author has been designated as the corresponding author with contact details:

• E-mail address

sham.rane.1@city.ac.uk

• Full postal address

CLG 34, Tait Building,
Northampton Square,
School of Engineering and Mathematical Sciences,
Centre for Positive Displacement Compressor Technology,
CITY University London,
London EC1V 0HB
England, UK

• Telephone and fax numbers

Phone: +44 (0) 20 70408395, +4407404455528
Fax: +44 (0) 20 7040 8566

All necessary files have been uploaded, and contain:
Highlights,
Manuscript,
Keywords,
All figures,
Figure captions,
All tables,
References.

• Manuscript has been 'spell-checked' and 'grammar-checked'
• References are in the correct format for this journal
• All references mentioned in the Reference list are cited in the text, and vice versa
• Permission has been obtained for use of copyrighted material from other sources – N/A
• Color figures are clearly marked as being intended for color reproduction on the Web (free of charge) and in print, or to be reproduced in color on the Web (free of charge) and in black-and-white in print.

IJR_Sham_CITY_2013_Resub_v1.doc
Click here to view linked References

Grid Deformation Strategies for CFD Analysis of Screw Compressors

Sham Rane*, Ahmed Kovacevic, Nikola Stosic, Madhulika Kethidi
City University London, Centre for Positive Displacement Compressor Technology,
London, EC1V 0HB, United Kingdom. E-mail: sham.rane.1@city.ac.uk
Phone: +442070408395, * Corresponding Author

ABSTRACT

Customized grid generation of twin screw machines for CFD analysis is widely used by the refrigeration and air-conditioning industry today, but is currently not suitable for topologies such as those of single screw, variable pitch or tri screw rotors. This paper investigates a technique called key-frame re-meshing that supplies pre-generated unstructured grids to the CFD solver at different time steps. To evaluate its accuracy, the results of an isentropic compression-expansion process in a reciprocating piston cylinder arrangement have been compared. Three strategies of grid deformation; diffusion equation mesh smoothing, user defined nodal displacement and key-frame remeshing have been assessed. There are many limitations to key-frame re-meshing. It requires time consuming pre-processing, has limited applicability to complex meshes and leads to inaccuracies in conservation of calculated variables. It was concluded that customized tools for generation of CFD grids are required for complex screw machines

Keywords: Twin Screw Compressor, CFD, Space Conservation, Deforming grids, Key-Frame Re-meshing.

Highlights:

- Key-Frame Grid Re-meshing investigated for Screw compressor CFD modeling.
- Accuracy of calculation evaluated through analysis of an isentropic process in a Piston-Cylinder.
- Successful use of customized grid generator demonstrated for twin screw compressor CFD analysis.
- The need for development of customized grid generators for multi-rotor screw machines highlighted.

NOMENCLATURE

CV	control volume	Ω	Volume of CV
S	Surface enclosing CV	$\boldsymbol{n}$	Unit vector orthogonal to S directed outwards
$\boldsymbol{v}$	Fluid velocity inside CV in a fixed coordinate system	ρ	Fluid density
t	Time	ϕ	Scalar transported in CV
Γ	Diffusivity for the quantity ϕ	q_ϕ	Source or Sink of ϕ in the CV
δ	Nodal displacement	Γ_{disp}	Mesh stiffness
p	Absolute Pressure	V	Specific Volume
T	Temperature	FVM	Finite Volume Method
CFD	Computational Fluid Dynamics	PDE	Partial Differential Equations

Subscripts 1 and 2 denote fluid initial and final state

1. INTRODUCTION

Rotary Screw Compressors are commonly used in industrial refrigeration and air-conditioning. The invention of the Twin Screw concept dates back to 1878 by Heinrich Krigar in Germany, whereas Single Screw compressors, comprising a main rotor and two star rotors originated around 1962. *Zimmern* (1984) has presented an historical review of the oil-injection free Single Screw Compressors. Twin screw compressors are far more common than single screw compressors in standard refrigeration and air-conditioning systems. Due to the introduction of new refrigerants, the use of natural refrigerants and other means of reducing greenhouse gases, the trends in refrigeration and heat pump technology today are towards higher pressure applications. In such cases single screw compressors start to dominate due to higher load capacities and more flexible control system than a twin screw compressor. This trend may even lead to design of screw compressors with other rotor configurations than those currently used. Capability to analyze performance of such complex screw machines is prerequisite for their successful design and commercialization,

There have been a number of studies conducted to develop thermodynamic models for twin screw and single screw compressors. The use of such models has helped remarkably both to evaluate compressor performance and to optimize rotor profiles over a period of time. For twin screw compressors with oil free or oil injected operations,

Fujiwara et al. (1984), *Fukazawa et al*. (1980), *Sangfors* (1984), *Singh et al.* (1984 and 1988), *Dagang et al.* (1986), *Kauder et al.* (1994) presented computer models. *Stosic et al.* (1988) developed models by solving numerically the energy and mass differential equations from first principles. *Hanjalic* and *Stosic* (1997) presented design optimization using such models. *Fleming et al.* (1998) presented a model for the development and performance improvement of these machines. More recently a book on the mathematical modeling of twin screw compressor was published by *Stosic et al*. (2005). Similarly for Single screw compressors, *Bein* and *Hamilton* (1982), *Boblitt* and *Moore* (1984), *Jianhua* and *Guangxi* (1988), *Li* and *Jin* (2004) presented computer models of oil flooded single screw compressors. *Lundberg* and *Glanvall* (1978) presented similar models and also compared twin and single screw type of compressors at full load. Such thermodynamic models require additional efforts to represent the deforming working domains through volume and area curves which often lead to inaccuracies or inability to analyse specific phenomena. Computational Fluid Dynamics (CFD) can be used to improve predictions on both aspects.

CFD is commonly based on Finite Volume Method (FVM) solvers. Their application to screw compressors involves unsteady flow with moving boundaries. The FVM has been used to solve problems involving unsteady flow with moving boundaries for a long time, as shown by *Peric* (1985), *Demirdzic* and *Peric* (1990), and *Demirdzic* and *Muzaferija* (1995). When the FVM is applied to screw compressors, the major problem is to form the grids required for transient simulations. During the operation of a compressor, the fluid domain between them is deformed as the rotors turn. Thus the CFD grid also has to deform. At present, commercially available general grid generators are not suitable for full three dimensional transient simulations of screw compressors, as shown by (*Kovacevic et. al.*, 2005, *Prasad*, 2004). A breakthrough was achieved in 1999 when the analytical rack generation method of *Stosic* (1998) was applied to generate an algebraic, adaptive, block – structured grid, used by *Kovacevic* (1999) for the calculation of twin screw rotor geometry. Since then there have been several reported uses of CFD analysis of twin screw compressor performance. *Kovacevic et al*, (1999 and 2000) and *Kovacevic* (2005) have presented the grid generation aspects for twin screw compressors. *Kovacevic et al*. (2002, 2003, 2006 and 2007) have reported CFD simulations of twin screw machines for predicting flow, heat transfer, fluid-structure interaction, etc. *Kovacevic et al.* (2007) also published a textbook on the three dimensional CFD analysis of screw compressors. *Voorde et al*. (2005) have developed a grid conversion algorithm for unstructured to block–structured mesh from the solution of the Laplace equation for twin screw compressors and pumps. Apart from these works, there are only a few reports available on transient three dimensional CFD analyses of screw machines. All these developments were concentrated on twin

screw compressors and so far there are no published works available on single screw machines or other complex screw machines such as those shown in Figure 1.

Figure 1 Screw Compressors with complex multi-rotor configurations (*Gardner*, 1969, *Nilsson*, 1949, *Zimmern*, 1984)

In this paper the fundamental aspects of transient CFD formulation with deforming grids are highlighted in order to emphasize importance of the technique used for handling deforming numerical mesh. The grid deformation handling technique called key-frame re-meshing is compared with the diffusion equation based mesh smoothing available in most of contemporary CFD codes (*ANSYS*, 2011) and the user defined nodal displacements based grid deformation as described in (*Kovacevic*, 2007). Two cases with increasing geometric complexity of the working chambers are studied, namely an isentropic compression-expansion process in a reciprocating piston cylinder arrangement and the twin screw compressor which proved to be extremely challenging for key-frame re-meshing.

2. FUNDAMENTALS OF CFD CALCULATION WITH DEFORMING BOUNDARIES

2.1 Laws of conservation and governing equations

In an Eulerian reference, the conservation of mass, momentum, energy and other intensive properties applied to fluid flow in a control volume (CV) can be defined by coupled, time dependent, partial differential equations.

Conservation of Scalar Quantities can be represented by a general transport equation, (*Ferziger* and *Peric*, 1996)

$$\underset{transient}{\frac{\partial}{\partial t}\int_{\Omega}\rho\phi d\Omega} + \underset{convection}{\int_{S}\rho\phi\boldsymbol{v}.\boldsymbol{n}dS} = \underset{diffusion}{\int_{S}\Gamma\ grad\ \phi.\boldsymbol{n}dS} + \underset{source}{\int_{\Omega}q_{\phi}d\Omega} \qquad (01)$$

When the control volume is not fixed in space, the solution domain changes with time due to movement of the boundaries. This movement is defined either as a function of time or is dependent on the current solution field. The convective fluxes such as the mass flux are calculated in these cases using relative velocity components at each cell face. If the coordinate system remains fixed and Cartesian velocity components are used, the only change in the conservation equation is the appearance of the relative velocity $(\boldsymbol{v}-\boldsymbol{v_b})$ in all convective terms, where $\boldsymbol{v_b}$ is the velocity vector at the cell face.

$$\frac{\partial}{\partial t}\int_{\Omega}\rho\phi d\Omega = \frac{d}{dt}\int_{\Omega}\rho\phi d\Omega - \int_{S}\rho\phi \boldsymbol{v_b}.\boldsymbol{n}dS \tag{02}$$

$$\underbrace{\frac{d}{dt}\int_{\Omega}\rho\phi d\Omega}_{transient} + \underbrace{\int_{S}\rho\phi(\boldsymbol{v} - \boldsymbol{v_b}).\boldsymbol{n}dS}_{convection} = \underbrace{\int_{S}\Gamma\ grad\ \phi.\boldsymbol{n}dS}_{diffusion} + \underbrace{\int_{\Omega}q_{\phi}d\Omega}_{source} \tag{03}$$

The application of Leibnitz's rule (02) for differentiation under the integral sign to transient terms of equation (01) gives the integral form of the general conservation equation. The grid velocity $\boldsymbol{v_b}$ and the grid motion are independent of the fluid motion. However, when the cell faces move and if the grid velocities are calculated explicitly and, in turn, used to calculate the convective fluxes, the conservation of mass and other conserved quantities are not necessarily preserved. To ensure full conservations of these equations, the space conservation law needs to be satisfied.

Space conservation or geometric conservation is given by,

$$\frac{d}{dt}\int_{\Omega}d\Omega - \int_{S}\boldsymbol{v_b}.\boldsymbol{n}dS = 0 \tag{04}$$

Space conservation can be regarded as mass conservation with zero fluid velocity. The unsteady terms in the governing equations involving integration over a control volume Ω, which is now changing with time, need to be treated in a way consistent with the space conservation equation with a deforming and/or moving grid. The grid velocities and changes in CV volumes are to be calculated in such way that equation (04) is not violated. If the first order backward differencing is used for temporal discretization, the transient term can be discretized as:

$$\frac{d}{dt}\int_{\Omega}\rho\phi d\Omega = \frac{(\rho\phi\Omega)^{n+1} - (\rho\phi\Omega)^{n}}{\Delta t} \tag{05}$$

Where, n and $n+1$ represent the current and next time level respectively. The $n+1$ volume Ω^{n+1} is computed from

$$\Omega^{n+1} = \Omega^{n} + \frac{d\Omega}{dt}\Delta t \tag{06}$$

Where, $d\Omega/dt$ is the rate of change of volume of CV and, in order to satisfy equation (04), it is calculated as

$$\frac{d\Omega}{dt} = \int_S \boldsymbol{v_b}.\boldsymbol{n}dS = \sum_j^{n_f} \boldsymbol{v_{b,j}} \cdot S_j \tag{07}$$

n_f is the number of faces on the control volume and S_j is the j^{th} face area vector. The dot product $\boldsymbol{v_{b,j}} \cdot S_j$ on each control volume face is calculated from the volume swept out $-\partial\Omega_j$ by that face over the time step Δt as $\partial\Omega_j/\Delta t$. Therefore the mass flux $\dot{m}_j$ can be calculated using $\partial\Omega_j/\Delta t$ instead of the explicitly calculated grid velocity $\boldsymbol{v_{b,j}}$.

$$\dot{m}_j = \int_{S_j} \rho(\boldsymbol{v} - \boldsymbol{v_{b,j}}).\boldsymbol{n}dS_j \approx \rho_j(\boldsymbol{v}.\boldsymbol{n})_j S_j - \frac{\rho_j \partial\Omega_j}{\Delta t} \tag{08}$$

If the volume change and mass fluxes are calculated as described above, space conservation is preserved. The requirement of space conservation in flow equations on moving integration points was introduced by *Thomas* and *Lombard* (1979). The importance of the space conservation law was discussed by *Demirdzic* and *Peric* (1988). They showed that the error in mass conservation due to nonconformance of space conservation is proportional to the time step size for constant grid velocities and is not influenced by the gird refinement size.

Theoretically, when the equations of conservation are integrated over control volumes of infinitesimal size they can completely resolve the flow dynamics. But when applied to control volumes of finite dimensions there are limitations in terms of resolving length scales beyond a certain size or capturing near wall boundary layer phenomena or shocks, where the gradients are high. So usually, in addition to these equations there can be more models introduced into the calculation, like turbulence models, near wall functions, species transport etc. These models can be analogously represented by the general transport equation and are not discussed here.

It is also possible to change the grid topology from one time step to another (*Ferziger* and *Peric*, 1996) since the computation of surface and volume integrals is not dependent on solution from previous time steps. This concept has been tested here to solve for complex domain deformations of screw compressors.

2.2 Solution of governing equations

The governing equations form a closely coupled, time dependent set of PDE's and commonly employ a Finite Volume Method for their solution.

Figure 2 Flow Chart of Solution Process with Deforming Domains

Figure 2 represents a flow chart of the solution process for a FVM with deforming domains. The solver used in this analysis is a pressure based coupled solver which solves for pressure based on the balancing of mass and momentum conservation. For compressible flows, where the density varies, the product of density and velocity in the mass conservation equation is linearized in terms of pressure. Hence a hydrodynamic system of equations, involving three Cartesian velocity components and pressure, is solved for every iteration in a time step. The highlighted block named 'Solve Mesh Displacement" in Figure 2 is of interest for this work. This step should allow for the movement of the initial grid to the new position in time, during which a control volume deforms. The mesh should retain the same number of nodes and cells while the cell deformation should be defined by the movement of its nodes. The integration process and the solution of the governing equations, as described in the previous section, will ensure that the space conservation is retained at the new time instance. The node displacement can be solved using different strategies, for example a) Spring smoothing, b) Diffusion equation smoothing or c) User defined nodal displacements through external subroutines.

In the diffusion equation based mesh smoothing (b), the specified displacement on the boundary nodes is propagated to the interior nodes by solving equation (09) internally in the solver.

$$\nabla \cdot \left(\Gamma_{disp} \nabla \delta\right) = 0 \tag{09}$$

Here, Γ_{disp} is the mesh stiffness that depends on local cell volumes and the distance of the nodes from the deforming boundaries. This method is presented graphically in Figure 3.

Figure 3 Grid Deformation using Diffusion Equation Mesh Smoothing

The number of cells and their connectivity remain constant for the duration of the calculation with the grid being deformed at the beginning of each time step. Mesh smoothing method is not suitable for large boundary displacements as it produces cells with high skewness and there are chances of element failure due to negative volumes after high nodal displacements. This limitation is dependent on the type of cells, the grid size relative to the magnitude of the boundary displacement, the relative orientation of the cells and the boundary displacement, the position of the non-deforming boundaries etc. For example, for tetrahedral types of cell the skewness quality

degrades faster with boundary displacements, compared to hexahedral cells. Hence for cases with simple geometries like a piston-cylinder this method can be used even with large displacements with hexahedral grids, but it fails for complex geometries like screw compressors.

Figure 4 Grid Deformation using User Defined Nodal Displacement

Customized grid generators can be used to generate a set of grids representing nodal locations for every time step externally, prior to numerical solution of flow in the calculation domain. The numerical grid is replaced at the beginning of each time step by use of appropriate user subroutines, often called 'Junction Boxes'. This method is called User Defined Nodal Displacement (c) and is shown graphically in Figure 4. In principle, it achieves the same result as the Diffusion Equation Mesh Smoothing but it is suitable for large boundary displacements because the nodal positions are controlled externally.

Figure 5 Grid Deformation using Key-Frame Grid Re-Meshing

Figure 5 shows another strategy suitable for high grid deformations which uses general purpose grid generators. Here, after every time step, Diffusion Smoothing is performed to obtain the new geometry. A check is then performed to determine whether the control volume cells can absorb further deformation without generating negative volume elements. Upon the discovery of irregular cells, groups of cells are selectively re-meshed locally, retaining the boundary geometry but with a change in the number of cells and their connectivity. This process is called Key-Frame re-meshing (*ANSYS*, 2011). Re-meshing is followed by the next time step calculations similar to those in Figure 2 but an intermediate interpolation of the solution from the previous time step is required because generally all cells will have changed connectivity. In this paper an attempt was made to use this algorithm for screw compressor applications.

3. CASE STUDIES

Two cases were studied to help assess the applicability of the key-frame re-meshing method to screw compressor simulations. In the first case, reversible adiabatic compression process in a piston cylinder was solved by use of the

diffusion smoothing, user defined nodal displacements and key-frame grid re-meshing techniques described above. This case was chosen as it forms the fundamental mechanism for calculating performance by CFD in positive displacement machines. The second case was a twin screw compressor with complex moving boundaries and highly deforming domains of both male and female rotors. In this case the key-frame grid re-meshing method was compared with the User defined nodal displacement provided by a customized grid generator.

3.1 Simulation of a simple Piston Cylinder Configuration

The purpose of this analysis was to compare the results from Diffusion smoothing based mesh deformation, User defined nodal displacements based mesh deformation and the Key-frame based re-meshing method with the theoretical results. Consider a piston cylinder arrangement with a sinusoidal displacement given to the piston.

Isentropic compression-expansion process in a reciprocating piston cylinder can be modeled by the polytropic process equation relating the gas pressure and volume. Since the process is adiabatic and reversible there will be no energy loses or gains in the control volume and the gas will return to its initial state.

$$\left(\frac{p_2}{p_1}\right) = \left(\frac{V_1}{V_2}\right)^{\gamma} = \left(\frac{T_2}{T_1}\right)^{\frac{\gamma}{(\gamma-1)}} \tag{10}$$

For this trial, a cylinder with diameter 100 mm and length 100 mm was considered. The initial position of the piston was for a maximum volume of 7.854×10^{-4} m^3. The Piston displacement was 70 mm varying sinusoidally with a frequency of 50Hz. The final minimum cylinder volume was 2.356×10^{-4} m^3. This gave a fixed volume ratio of 3.333 for the system. Based on equation (10), for an initial absolute pressure in the cylinder of 2.013 bar the expected peak pressure is 10.86 bar. Similarly, for an initial temperature of 298 K, the expected peak temperature is 482.35 K.

In order to make the CFD model isentropic, all boundaries were defined as adiabatic and calculation of viscous dissipation term in the conservation equation of total energy was turned off. This also took account of the turbulent viscosity dissipation factor.

Figure 6 Hexahedral Mesh at different time steps using Diffusion Smoothing (SH1)

The most suitable configuration for diffusion smoothing is a hexahedral mesh since the cell quality does not deteriorate much when boundaries deform. Figure 6 shows the hexahedral mesh generated by diffusion smoothing at

three different time steps. The hexahedral meshes generated by diffusion smoothing were identified as **SH**. The mesh shown in Figure 6 is a coarse mesh consisting of 22752 cells identified as **SH1**. Two refined meshes were generated by the same method and named **SH2** consisting of 49962 cells and **SH3** consisting of 74720 cells (Table 1).

For the key-frame based re-meshing a tetrahedral mesh was selected, as shown in Figure 7. Three different cases were generated, namely coarse **KR1**, medium **KR2** and fine **KR3** consisting of similar number of cells and nodes (Table 1).

For the User Defined Nodal Displacement, a Hexahedral mesh was selected and three grid sizes were generated to correspond to sizes of the Diffusion smoothing. These were named **UH1**, **UH2** and **UH3** respectively, as listed in Table 1.

The time step was 2.8571×10^{-4} sec while each cycle contained 70 time steps which corresponded to 50 cycles per second. The mesh deformation was applied after each time step. The implicit second order backward Euler discretization was used within the pressure based coupled solver. The advection scheme was high resolution and the turbulence model was k-epsilon. An r.m.s. residual target of 1.0×10^{-4} was maintained for all equations. The fluid was air assumed to be an ideal gas with the molar mass of 28.96 kg $kmol^{-1}$, Specific Heat Capacity 1004.4 J kg^{-1} K^{-1}, Dynamic Viscosity 1.831×10^{-5} kg m^{-1} s^{-1} and Thermal Conductivity 2.61×10^{-2} W m^{-1} K^{-1}.

Figure 7 Tetrahedral Mesh at different time steps used in key-frame re-meshing (KR1)

Figure 8 Piston Displacement with Diffusion smoothing (SH1) and key-frame re-meshing (KR1)

Figure 9 Pressure history of diffusion smoothing (SH1) and key-frame re-meshing (KR1)

Figure 10 Temperature history of diffusion smoothing (SH1) and key-frame re-meshing (KR1)

Figure 8 shows the variation of piston displacement with time for the same volume ratio in cases SH1 and KR1. Figure 9 shows the change of pressure with time in cases SH1 and KR1. The results obtained with Nodal displacement UH1 were identical to that of SH. All case grid details and results are presented in Table 1. Although both, diffusion smoothing SH1 and key-frame re-meshing KR1 follow the same change of volume during compression and expansion, the calculated peak pressures are not equal. In the case of diffusion smoothing the

pressure in the first cycle achieved the theoretical peak of 10.86 bar and consistently repeated itself in the following cycles. But in the case of key-frame re-meshing the maximum pressure in the first cycle was higher than the theoretical value and it continued to increase in the following cycles. Similarly the initial state of pressure at the end of expansion did not return to its base value as it did in the case of diffusion smoothing. Figure 10 shows the temperature change with time in the cylinder for both cases. The peak temperatures are not equal in the two cases. In the case of diffusion smoothing the temperature in the first cycle rises to the theoretical peak of 482.35 K and repeats itself in the following cycles consistently. In the case of key-frame re-meshing the peak temperature in the first cycle is similar to the theoretical value but it continues to increase in the following cycles. Similarly the initial state of temperature, at the end of expansion does not return to its base level of 298 K as it does in the case of diffusion smoothing. Table 1 shows the error in the prediction of pressure and temperature obtained from the three different grid deformations strategieswith three different grid sizes and over multiple consecutive compression cycles.

Table 1: Mesh statistics and errors in results compared to theoretical values

Figure 11 Error in pressure predictions

Figure 12 Error in temperature predictions

The error in the pressure predictions over three consecutive compression cycles for the various grid deformation strategies is shown in Figure 11, while Figure 12 shows the error in the temperature calculation over the compression cycles for these three cases.

The results show that the Diffusion smoothing (SH) based method of grid displacement and User defined nodal displacement (UH) based method of grid displacement produce the same, highly accurate predictions which conform with the theoretical results for this deforming boundary formulation. However, errors in the pressure and temperature prediction exist when the key-frame re-meshing based method of grid deformation is used. For the key-frame re-meshing method, the error increases with grid refinement.

Since the mesh is replaced for each time step it is quite possible that space conservation is violated in the key-frame re-meshing method. This in turn induces an increase in calculation error. As pointed out in *Ferziger* and *Peric* (1996), this can lead to artificial mass source errors in the continuity equation that can also accumulate with flow time. Table 1 shows the error in mass over multiple consecutive compression cycles for the three different grid

deformation strategies. Limiting the mesh to be replaced, only when the cell quality is severely reduced, should help in reducing the error, but in the case of complex topologies, as in screw compressors, this is very difficult if not impossible.

3.2 Simulation of a Twin Screw Compressor

For the CFD analysis of twin screw machines, the customized grid generation tool is available as described in *Kovacevic et al.*, 2007. It allows numerical mesh generation of the deforming rotor domains by a hexahedral grid with a constant number of cells for each time step and unstructured stationary meshes of compressor ports. A set of grids for the entire compression cycle is then supplied to the solver. Figure 13 shows a simplified block diagram of the screw compressor rotor grid generation process. It decomposes the entire rotor domain into two sub-domains which are separated by the common line called a 'rack'. Each of these domains belongs to one of the rotors and is of an "O" topology.

Consecutive 2D cross sections are mapped individually through following steps (*Kovacevic et. al.*, 2003):

1. Transformation from the 'physical' domain to the numerical non-dimensional domain.
2. Definition of the edge nodes by applying an adaptive distribution technique.
3. Selection and matching of four non-contacting boundaries.
4. Calculation of the curves, which connect the facing boundaries by transfinite interpolation.
5. Application of a stretching function to obtain the distribution of the grid points.
6. Orthogonalisation, smoothing and final checking of the grid consistency.

This procedure allows the method of User defined nodal displacement to be implemented and is today an industrial standard widely used for screw compressors. The details of the algorithm have been presented by the authors in *Kovacevic et al.* (2007)

Figure 13 Simplified Block Diagram of Screw Compressor Rotor Grid Generation

An attempt was also made to apply key-frame grid re-meshing using a general purpose grid generator. Although not required for twin screw compressors it is an excellent case for comparison and complex enough to evaluate its use for variable pitch geometries or geometries with non-parallel axes which currently do not have a grid generation solution. The case study was performed on a 3/5 "N" rotor combination in an oil free twin screw compressor with a

male rotor diameter of 127mm. Initially, an attempt was made to generate a complete model for Key-frame re-meshing that included both radial and interlobe leakage gaps as shown in Figure 14. A very fine grid was generated to capture the clearances. It was found that for a male rotor speed of 8600rpm, the max displacement that could be given to the rotor was about 0.1 degree per time step before the formation of negative element volumes occurred. Therefore it was practically impossible to obtain a sufficient number of meshes and to perform this calculation. In the alternative second attempt the radial clearances were excluded. This further complicated the geometry as shown in Figure 15 after which it was concluded that the key-frame re-meshing could not be applied to the twin screw compressor geometry without excessive computing resource and time.

The user defined nodal displacement method was successfully applied and the case was solved with a pressure ratio of 2:1 at 8600rpm. The male rotor subdomain was mapped by 154860 cells and 172260 nodes. The female rotor subdomain was mapped with 160200 cells and 178200 nodes while the suction and discharge ports contained 855481 cell and 178446 nodes, respectively.

Figure 16 shows the variation of mass flow rate through the suction and discharge of the compressor and Figure 17 shows the absolute pressure contours. An error of about 2.19% is observed in the average mass balance between the suction and discharge flows. The error remains unchanged over a number of compressor cycles which indicates that it is not the consequence of a violation of the conservation law as in the case of key-frame re-meshing. There are two main reasons for the error. Firstly, even with a large number of cells, the grid generation technique employed for screw compressors nodal displacement with hexahedral cells produces a relatively coarse mesh along the sliding interface between two subdomains. Secondly, in the clearance gaps, the cells have a very large aspect ratio and are relatively coarse. Due to this, it was found to be very difficult to achieve a residual level below $1x10^{-4}$ r.m.s for every time step for the mass and momentum equations. However, it is expected that by continuing the calculation for a large number of cyclic repetitions, the accuracy will be improved as the flow stabilises in the connecting ports.

Kovacevic et al., (2002, 2003, 2005, 2006 and 2007) have reported CFD simulations of twin screw machines for the prediction of flow, heat transfer, fluid-structure interaction, and other applications, using the same grid generation tools. This method retains conservation of space fully and provides accurate results. Further developments of this method with particular attention to grid refinement in the clearances and along sliding interfaces will improve the accuracy.

Typically the pre-processing time required when using the key-frame re-meshing methodology is around 50 hours of machine time whereas, when using customized grid generation, it is not more than 2 hours. Importantly, leakage flows in the radial and interlobe clearances are captured. This case study showed limitations to the application of key-frame re-meshing to solve complex screw compressor problems.

Figure 14 Deforming rotor domain Including Leakage Clearances

Figure 15 Deforming rotor domain with Radial Leakage Excluded

Figure 16 Mass Flow Rate Variations at Suction and Discharge

Figure 17 Contours of Pressure variation

4. CONCLUSION

Successful simulation of reversible adiabatic compression in a Piston-Cylinder was carried out with three grid deformation methods; Diffusion Smoothing, User Defined Nodal Displacement and Key-Frame Re-meshing. Diffusion Smoothing and User Defined Nodal Displacement produced exactly the same results with accurate estimates of pressure and temperature. Key-Frame Re-Meshing method gave inconsistent results with increasing error in pressure and temperature predictions in successive compression cycles. Grid refinement did not improve the accuracy of Key-Frame Re-Meshing while reducing the time step made excessive demands on pre-processing.

All attempts to solve flow within a twin screw compressor by use of Key-Frame Re-meshing failed, due to the complexity of the numerical mesh. However, by applying User Defined Nodal Displacement, using a customized grid generator, it was possible to demonstrate a suitable method for grid deformation solution in screw compressor CFD analysis. Thus for future work, it will be necessary to develop customized tools to generate CFD grids for complex screw machines such as single screw, variable pitch machines and tri-rotor screw machines. These grids will facilitate grid deformation strategy of User Defined Nodal Displacement in the solvers.

REFERENCES

ANSYS 13.0, 2011, User Guide and Help Manual.

Bein T. W., Hamilton J F., 1982, Computer modeling of an oil flooded Single Screw Compressor. *Proc Int Compressor Conf at Purdue*, Paper 383.

Boblitt W. W. and Moore J., 1984, Computer Modeling of Single -Screw Oil Flooded Refrigerant Compressors, *Proc. Int. Compressor Conf. at Purdue*, Paper 506.

Dagang X., Xion Z., Yu Y., 1986, The Computer Simulation of Oil Flooded Refrigeration Twin-Screw Compressor, *Proc. Int. Compressor Conf. at Purdue*, Paper 345

Demirdzic I., Muzaferija S., 1995, Numerical Method for Coupled Fluid Flow, Heat Transfer and Stress Analysis Using Unstructured Moving Mesh with Cells of Arbitrary Topology, *Comp. Methods Appl. Mech. Eng.*, Vol.125, pp. 235-255

Demirdzic I., Peric M., 1990, Finite Volume Method for Prediction of Fluid flow in Arbitrary Shaped Domains with Moving Boundaries, *Int. J. Numer. Methods Fluids*, Vol.10, p. 771

Ferziger J. H. and Peric M., 1996, *Computational Methods for Fluid Dynamics*, ISBN 978-3-540-42074-3, Springer, Berlin, Germany.

Fleming J. S., Tang Y., Cook G., 1998, The Twin Helical Screw Compressor, Part 1: Development, Applications and Competitive Position, Part 2: A Mathematical Model of the Working process, *Proc. Inst. Mech. Eng. Part C, J. Mech. Eng. Sci.*, Vol. 212, p. 369.

Fujiwara M., Kasuya, K., Matsunaga, T. and Watanabe, M., 1984, Computer Modeling for Performance Analysis of Rotary Screw Compressor. *Proc. Int. Compressor Conf. at Purdue*, Paper 503.

Fukazawa Y., Ozawa U., 1980, Small Screw Compressors for Automobile Air Conditioning Systems. *Proc Int Compressor Conf at Purdue*, Paper 351.

Gardner J. W.,1969, US Patent No 3,424,373 – Variable Lead Compressor. Patented 1969.

Hanjalic K., Stosic N., 1997, Development and Optimization of Screw machines with a simulation Model – Part II: Thermodynamic Performance Simulation and Design Optimization. *ASME Transactions, Journal of Fluids Engineering*, 119: 664 – 670.

Jianhua Wu and Guangxi Jin, 1988, The Computer Simulation of Oil-Flooded Single Screw Compressors, *Proc. Int. Compressor Conf. at Purdue*, Paper 646.

Kauder K., Rau B., 1994, Auslegungsverfahren fur Schraubenkompressoren. (Design Procedure for screw compressors), VDI Berichte 1135, S. 31-44, Düsseldorf: VDI-Verlag.

Kovacevic A., Stosic N., Smith I. K., 1999, Development of CAD-CFD Interface for Screw Compressor Design, *International Conference on Compressors and Their Systems, London, IMechE Proceedings*, Paper C542-075, 757-767.

Kovacevic A., Stosic N., Smith I. K., 2000, Grid Aspects of Screw Compressor Flow Calculations, *Proceedings of the ASME Advanced Energy Systems Division, Orlando FL*, Vol. 40, pp. 83.

Kovacevic A., 2005, Boundary Adaptation in Grid Generation for CFD Analysis of Screw Compressors, *Int. J. Numer. Methods Eng.*, Vol. 64: 401-426.

Kovacevic A., Stosic N. and Smith I. K, 2002, Numerical Simulation of Fluid Flow and Solid Structure in Screw Compressors, *Proceedings of ASME Congress*, New Orleans, IMECE2002-33367.

Kovacevic A., Stosic N. and Smith I. K., 2003, Three Dimensional Numerical Analysis of Screw Compressor Performance, *Journal of Computational Methods in Sciences and Engineering*, 3: 259-284.

Kovacevic A., Stosic N., Smith I. K., 2006, Numerical simulation of combined screw compressor–expander machines for use in high pressure refrigeration systems, *Simulation Modeling Practice and Theory*, Vol. 14, 8, pp. 1143–1150.

Kovacevic A., Stosic N. and Smith I. K., 2007, *Screw compressors - Three dimensional computational fluid dynamics and solid fluid interaction*, ISBN 3-540-36302-5, Springer-Verlag Berlin Heidelberg New York.

Li Hong Qi and Jin Li Wen, 2004, Design Optimization of an Oil-Flooded Refrigeration Single Screw Compressor, *Proc. Int. Compressor Conf. at Purdue*, Paper 1715.

Lundberg A. and Glanvall R., 1978, A Comparison of SRM and Globoid Type Screw Compressors at Full Load, *Proc. Int. Compressor Conf. at Purdue*, Paper 288.

Nilsson H. R., 1949, US Patent No 2,481,527 – Rotary Multiple Helical Rotor Machine.

Peric, M., 1985, A Finite Volume Method for the Prediction of Three Dimensional Fluid Flow in Complex Ducts, *PhD Thesis, Imperial College of Science, Technology & Medicine*, London

Prasad, B. G. Shiva, 2004, CFD for Positive Displacement Compressors, *Proc. Int. Compressor Conf. at Purdue*. Paper 1689.

Sangfors B., 1984, Computer Simulation of the Oil Injected Twin Screw Compressor, *Proc. Int. Compressor Conf. at Purdue*, Paper 528.

Singh P. J., Onuschak A. D., 1984, A Comprehensive Computerized Method for Twin Screw Rotor Profile Generation and Analysis, *Proc. Int. Compressor Conf. at Purdue*. Paper 501.

Singh P. J., Schwartz J. R., 1988, Exact Analytical Representation of Screw Compressor Rotor Geometry. *Proc Int Compressor Conf at Purdue*, Paper 925.

Stosic N., Hanjalic K., Kovacevic A. and Milutinovic Lj, 1988, Mathematical Modeling of the Influence of Oil on the Working Cycle of Screw Compressors. *Proc. Int. Compressor Conf. at PurdueI*. Paper 645.

Stosic N., 1998, On Gearing of Helical Screw Compressor Rotors, *Proceeding of IMechE, Part C: J. Mech. Eng. Science*, Vol.212, and pp. 587.

Stosic N., Smith I.K. and Kovacevic A., 2005, *Screw Compressors: Mathematical Modeling and Performance Calculation*, Monograph, Springer Verlag, Berlin, June 2005, ISBN: 3-540-24275-9

Thomas P. and Lombard C., 1979, Geometric conservation law and its application to flow computations on moving grids, AIAA, 17, 1030–1037.

Voorde John Vande and Vierendeels Jan, 2005, A grid manipulation algorithm for ALE calculations in screw compressors. 17th AIAA Computational Fluid Dynamics Conference, Canada, AIAA 2005-4701.

Zimmern Bernard, 1984, From Water to Refrigerant: Twenty Years to Develop the Oil Injection-Free Single Screw Compressor. *Proc. Int. Compressor Conf. at Purdue,* Paper 500.

Figure Captions

Figure 1 Screw Compressors with complex multi-rotor configurations (*Gardner*, 1969, *Nilsson*, 1949, *Zimmern*, 1984)

Figure 2 Flow Chart of Solution Process with Deforming Domains

Figure 3 Grid Deformation using Diffusion Equation Mesh Smoothing

Figure 4 Grid Deformation using User Defined Nodal Displacement

Figure 5 Grid Deformation using Key-Frame Grid Re-Meshing

Figure 6 Hexahedral Mesh at different time steps using Diffusion Smoothing (SH1)

Figure 7 Tetrahedral Mesh at different time steps used in key-frame re-meshing (KR1)

Figure 8 Piston Displacement with Diffusion smoothing (SH1) and key-frame re-meshing (KR1)

Figure 9 Pressure history of diffusion smoothing (SH1) and key-frame re-meshing (KR1)

Figure 10 Temperature history of diffusion smoothing (SH1) and key-frame re-meshing (KR1)

Figure 11 Error in pressure predictions

Figure 12 Error in temperature predictions

Figure 13 Simplified Block Diagram of Screw Compressor Rotor Grid Generation

Figure 14 Deforming rotor domain including Leakage Clearances

Figure 15 Deforming rotor domain with Radial Leakage excluded

Figure 16 Mass Flow Rate Variations at Suction and Discharge

Figure 17 Contours of Pressure variation

Fig1.tif
Click here to download high resolution image

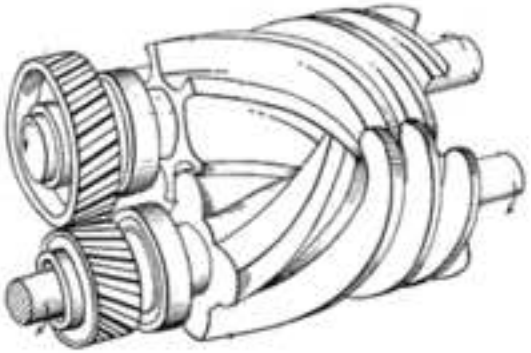

Variable Pitch Twin Screw

Cylindrical Screw – Planar Gaterotors

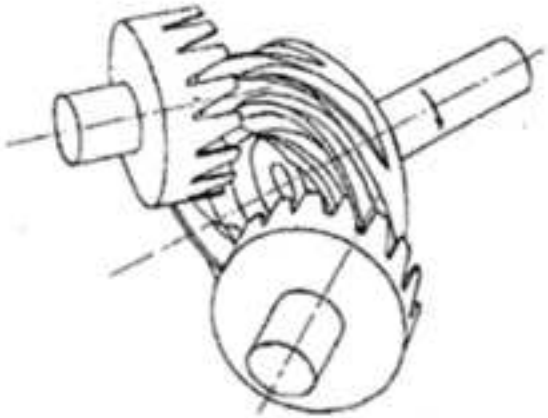

Planar Screw – Cylindrical Gaterotors

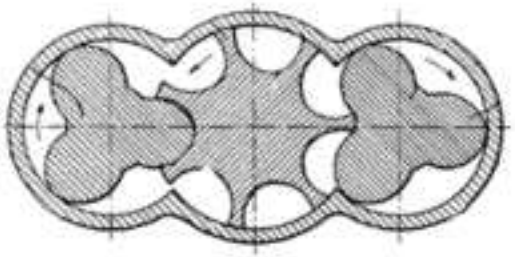

Tri-Rotor Screws

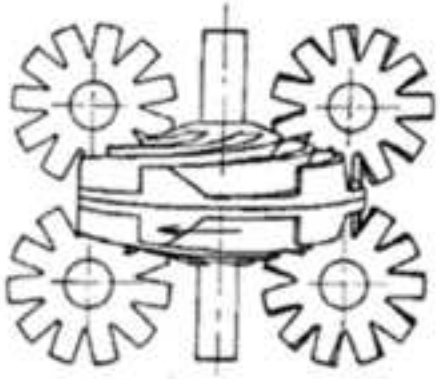

Planar Screw – Planar Gaterotors

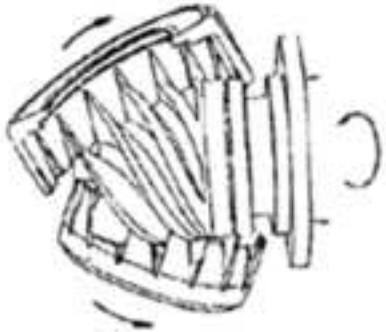

Cylindrical Screw – Cylindrical Gaterotors

Fig2.tif
Click here to download high resolution image

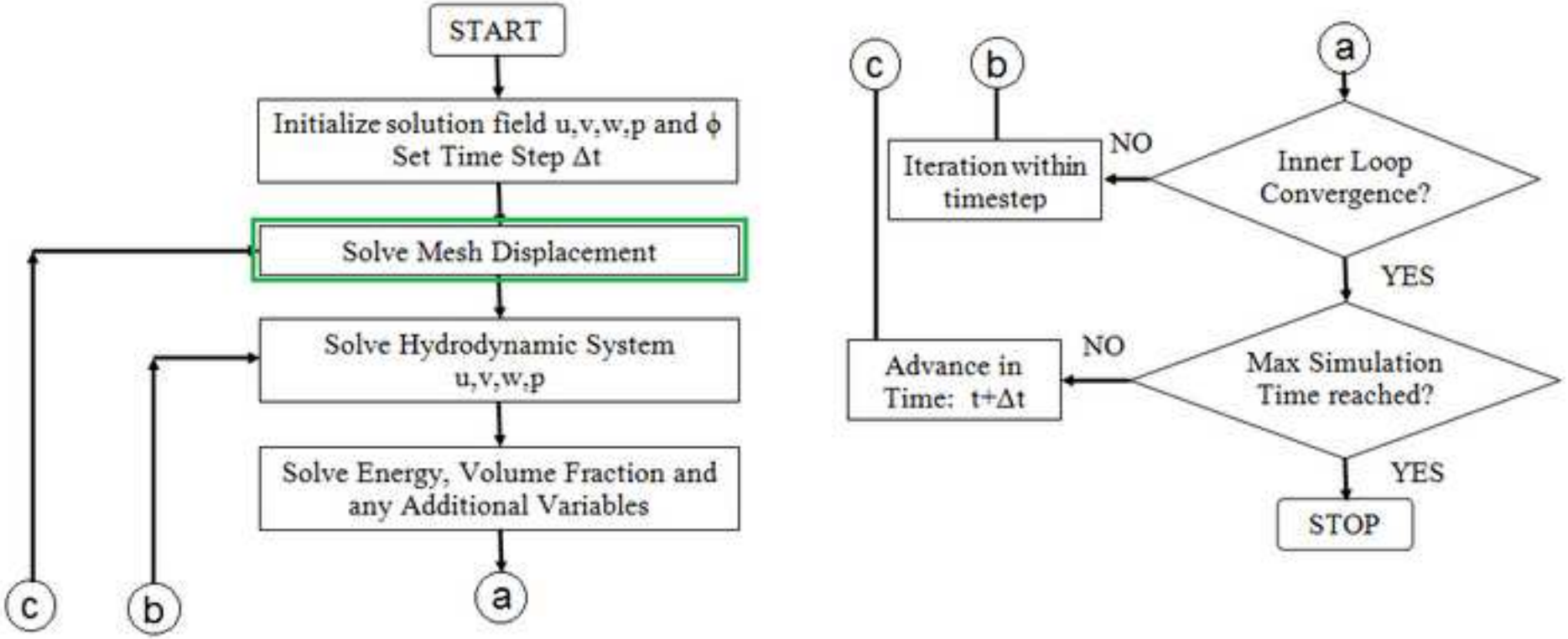

Fig3.tif
Click here to download high resolution image

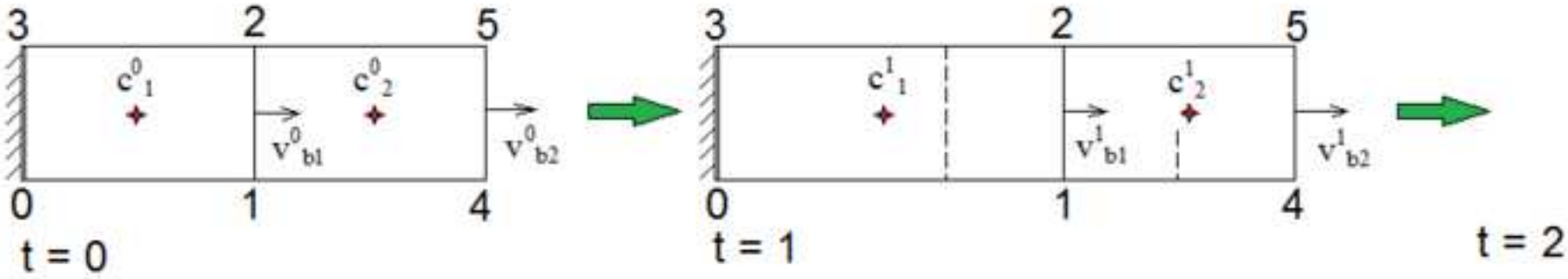

- δx4, δx5 – Specified
- δx1, δx2 – Calculated
- v^1_{b1}, v^1_{b2} – Calculated

$$\nabla \cdot \left(\Gamma_{disp} \nabla \delta \right) = 0$$

Fig4.tif
Click here to download high resolution image

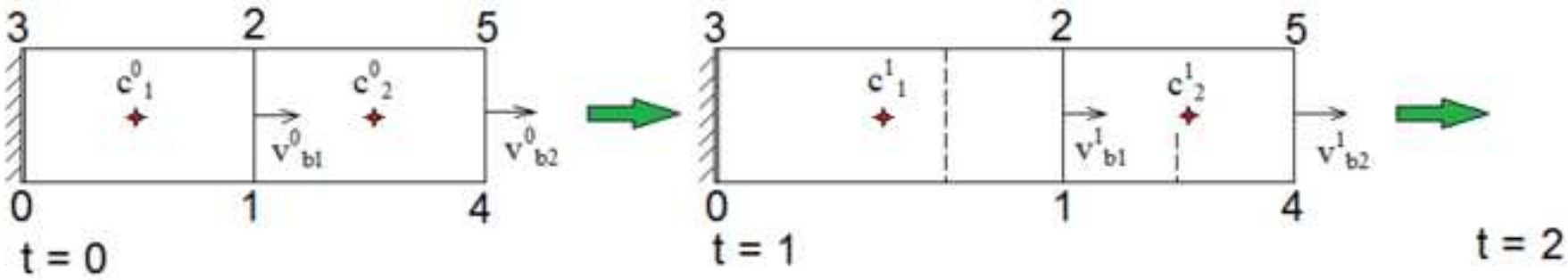

- δx1, δx2, δx4, δx5 – Specified
- v^1_{b1}, v^1_{b2} – Calculated

Fig5.tif
Click here to download high resolution image

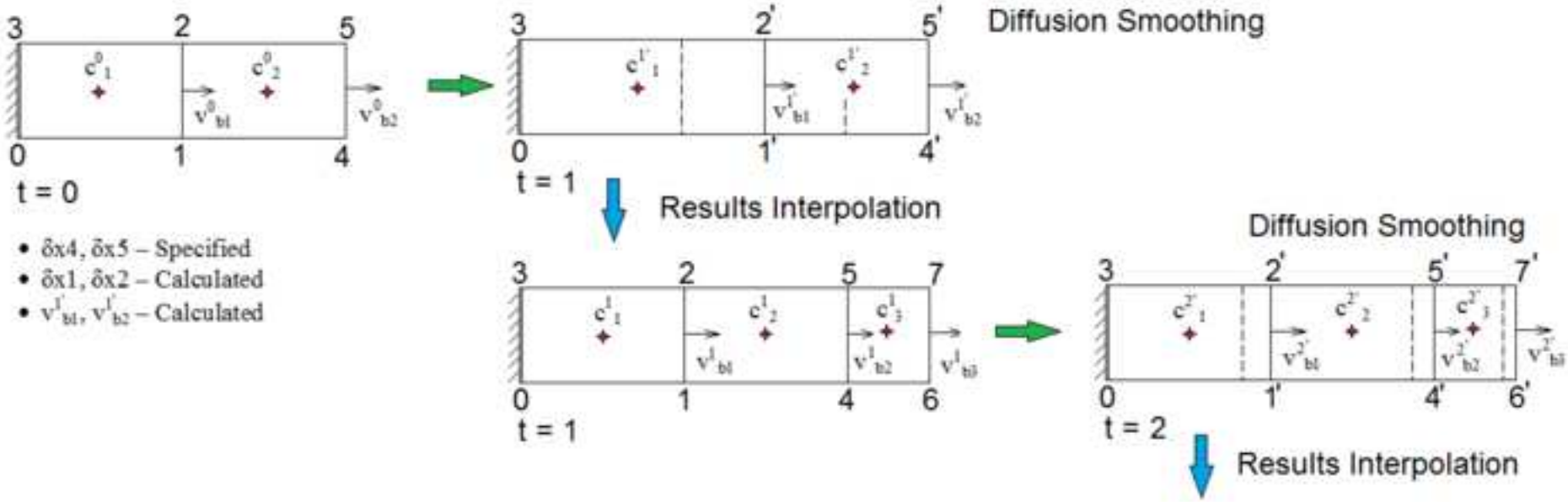

Fig6.tif
Click here to download high resolution image

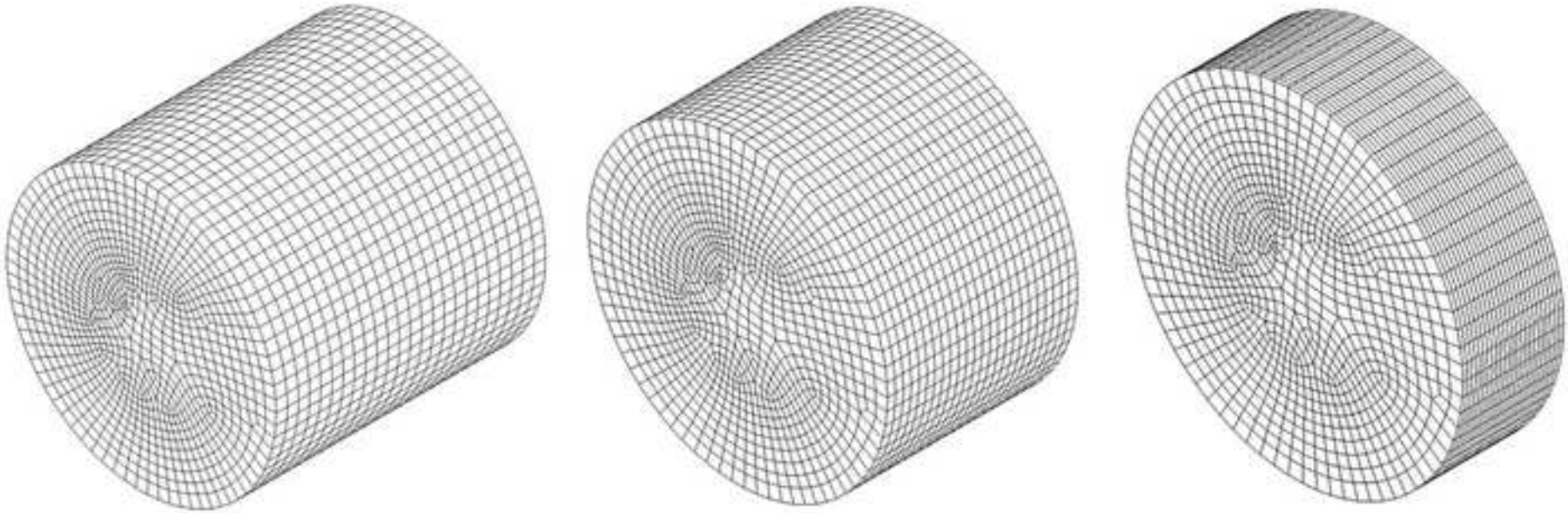

Fig7.tif
Click here to download high resolution image

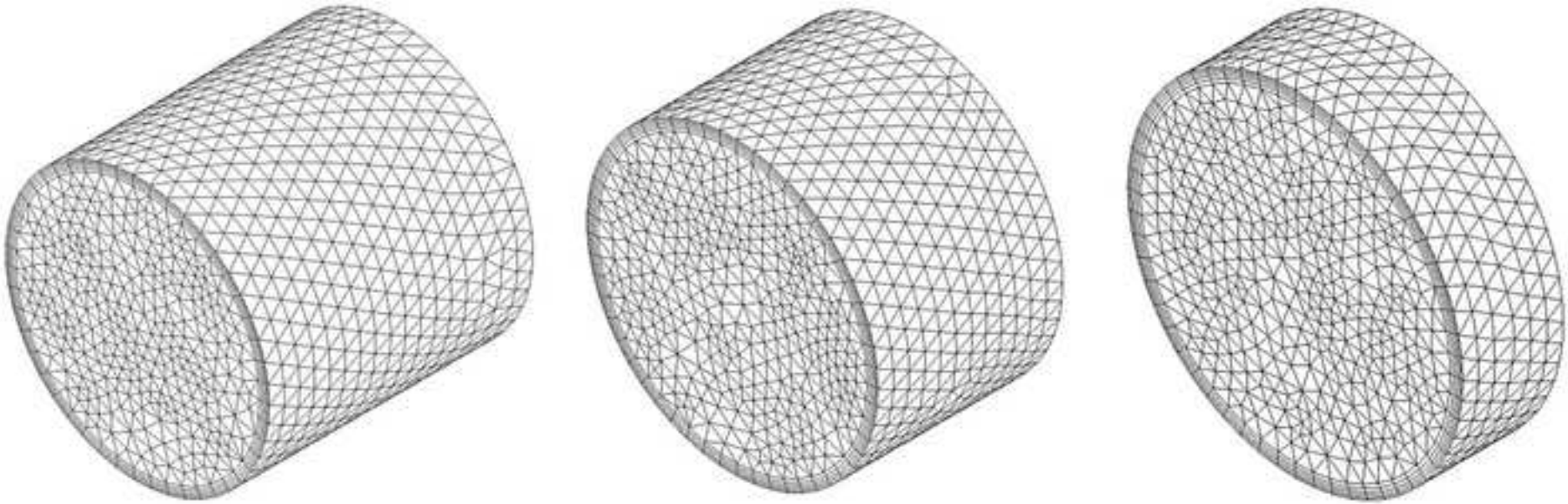

Fig8.tif
Click here to download high resolution image

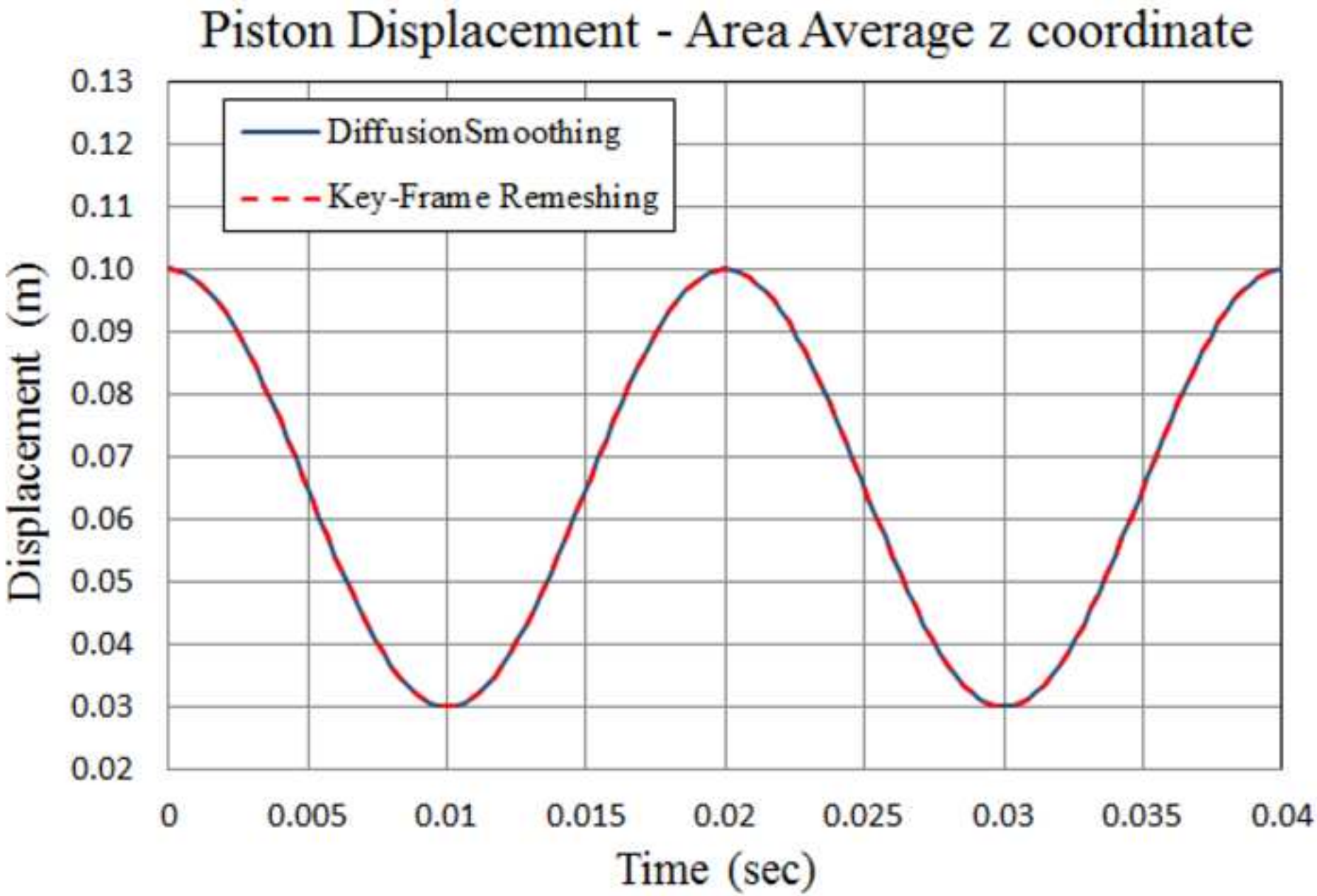

Fig9.tif
Click here to download high resolution image

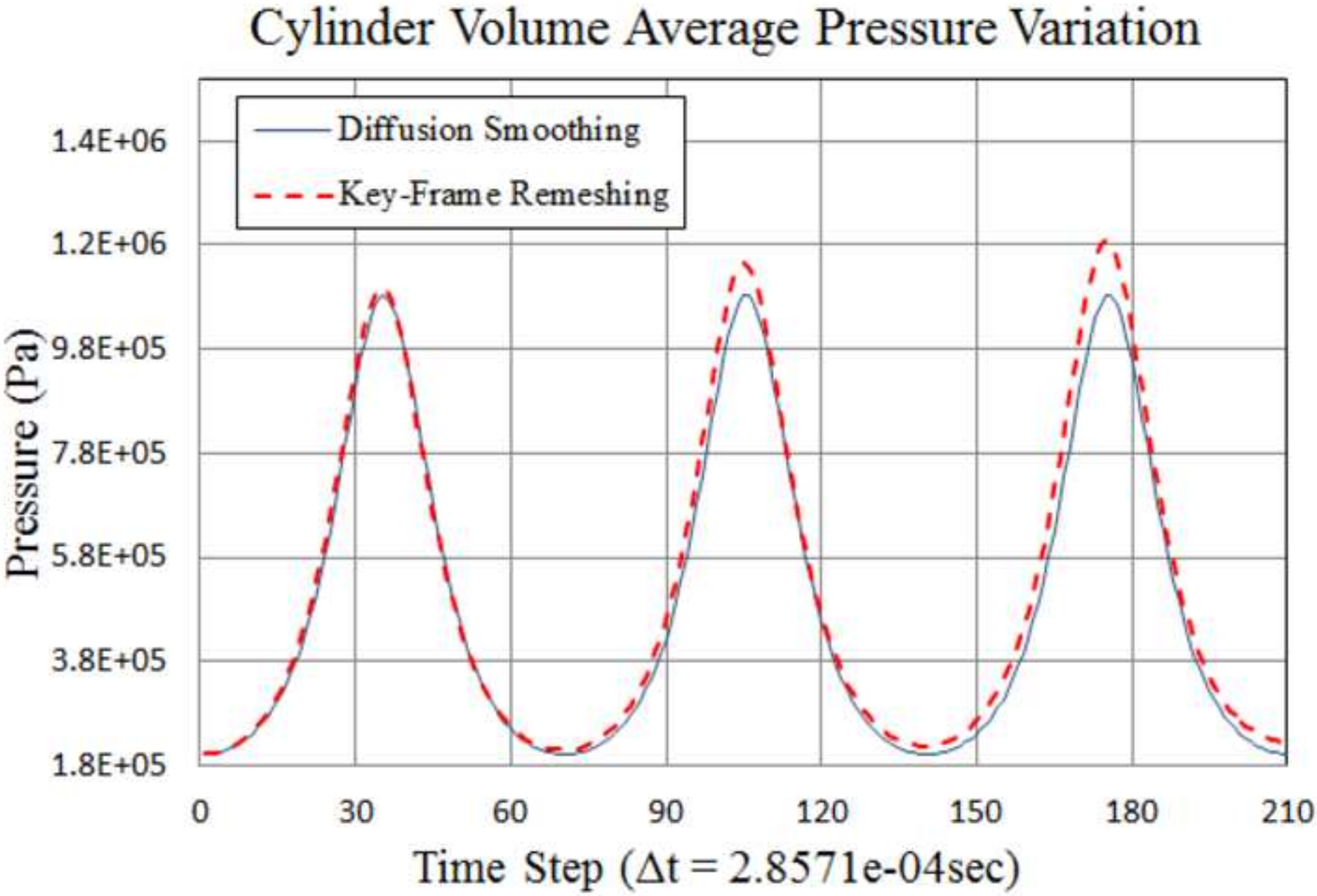

Fig10.tif
Click here to download high resolution image

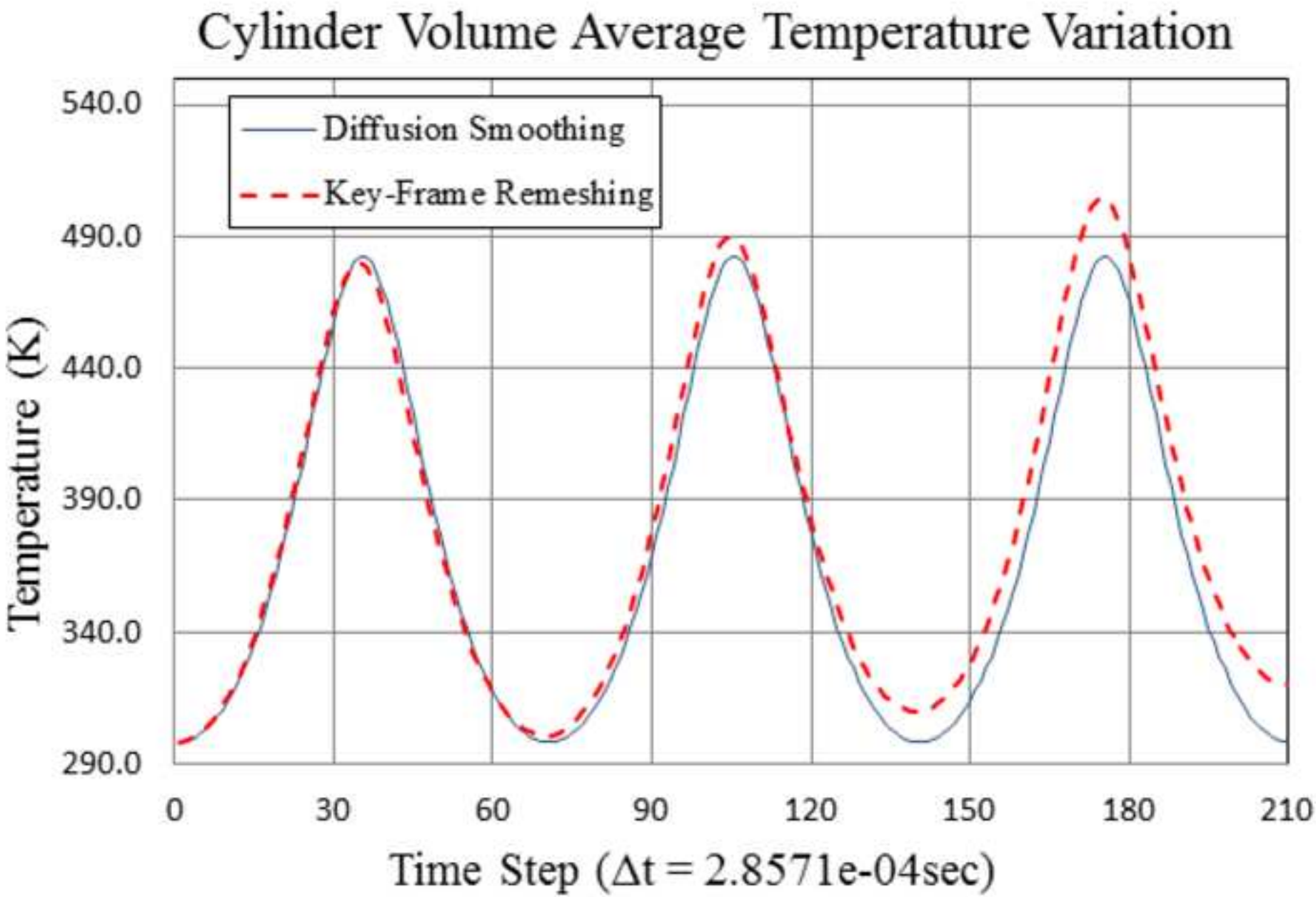

Fig11.tif
Click here to download high resolution image

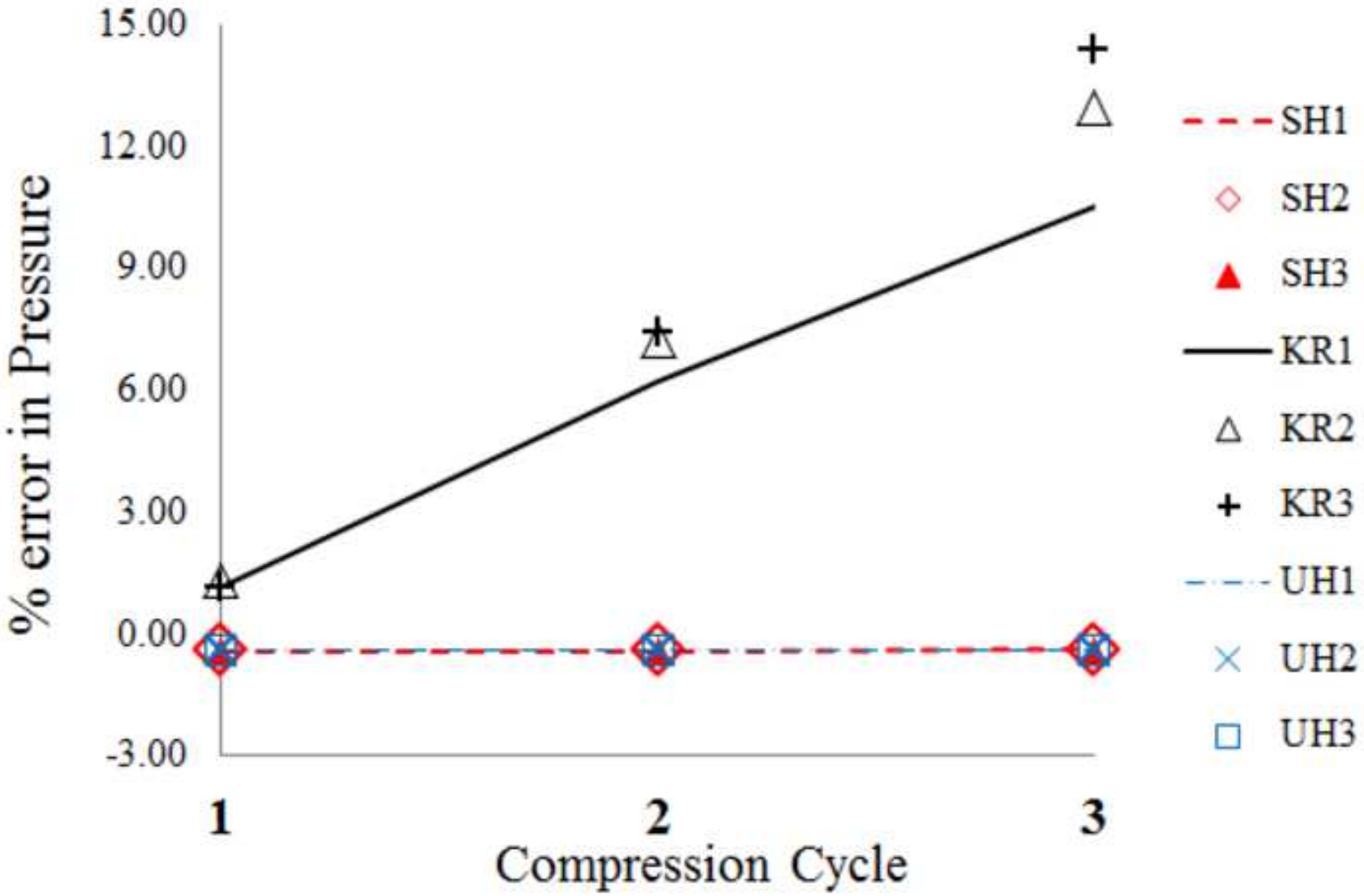

Fig12.tif
Click here to download high resolution image

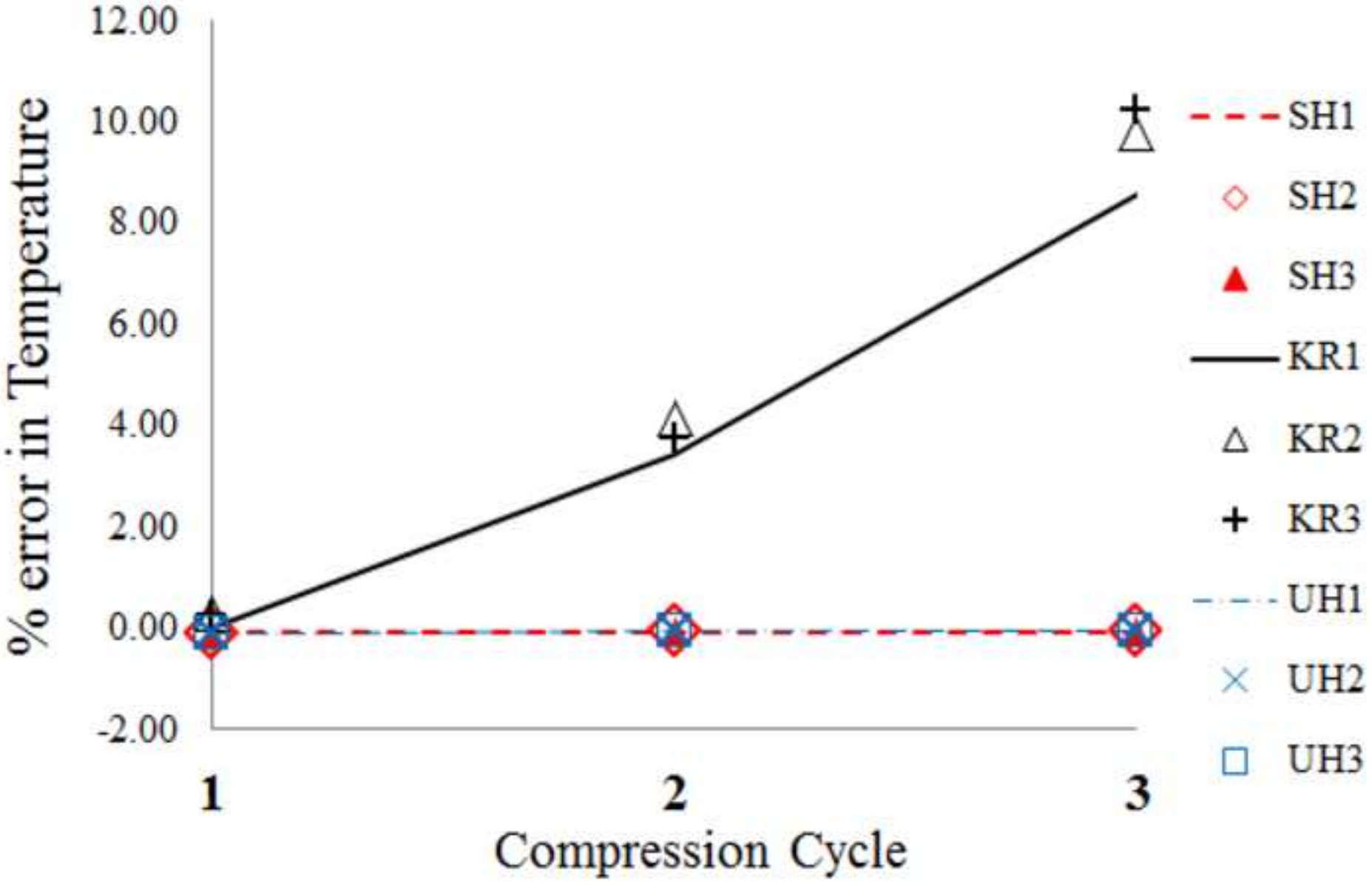

Fig13.tiff

Click here to download high resolution image

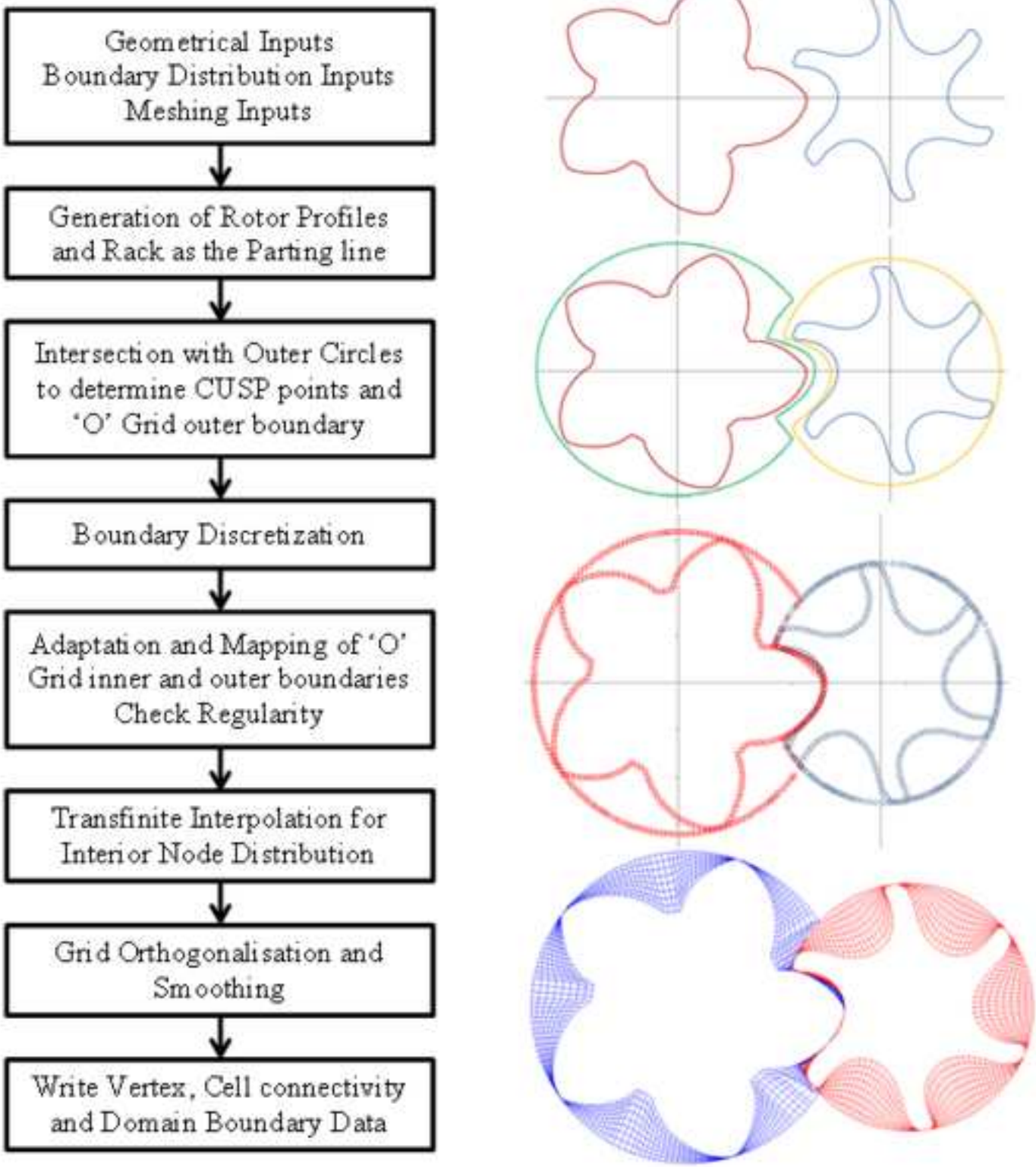

Fig14.tiff

Click here to download high resolution image

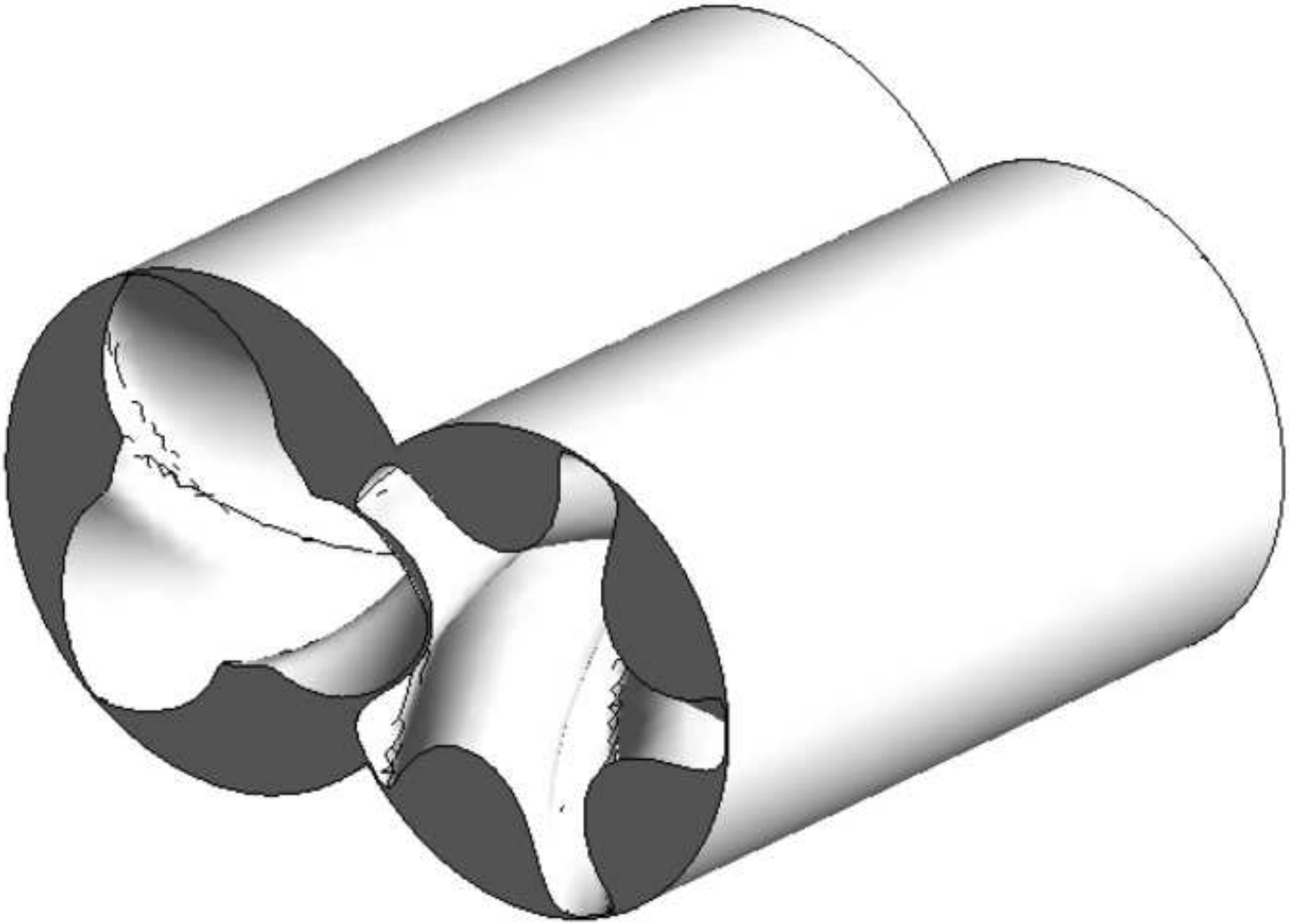

Fig15.tiff

Click here to download high resolution image

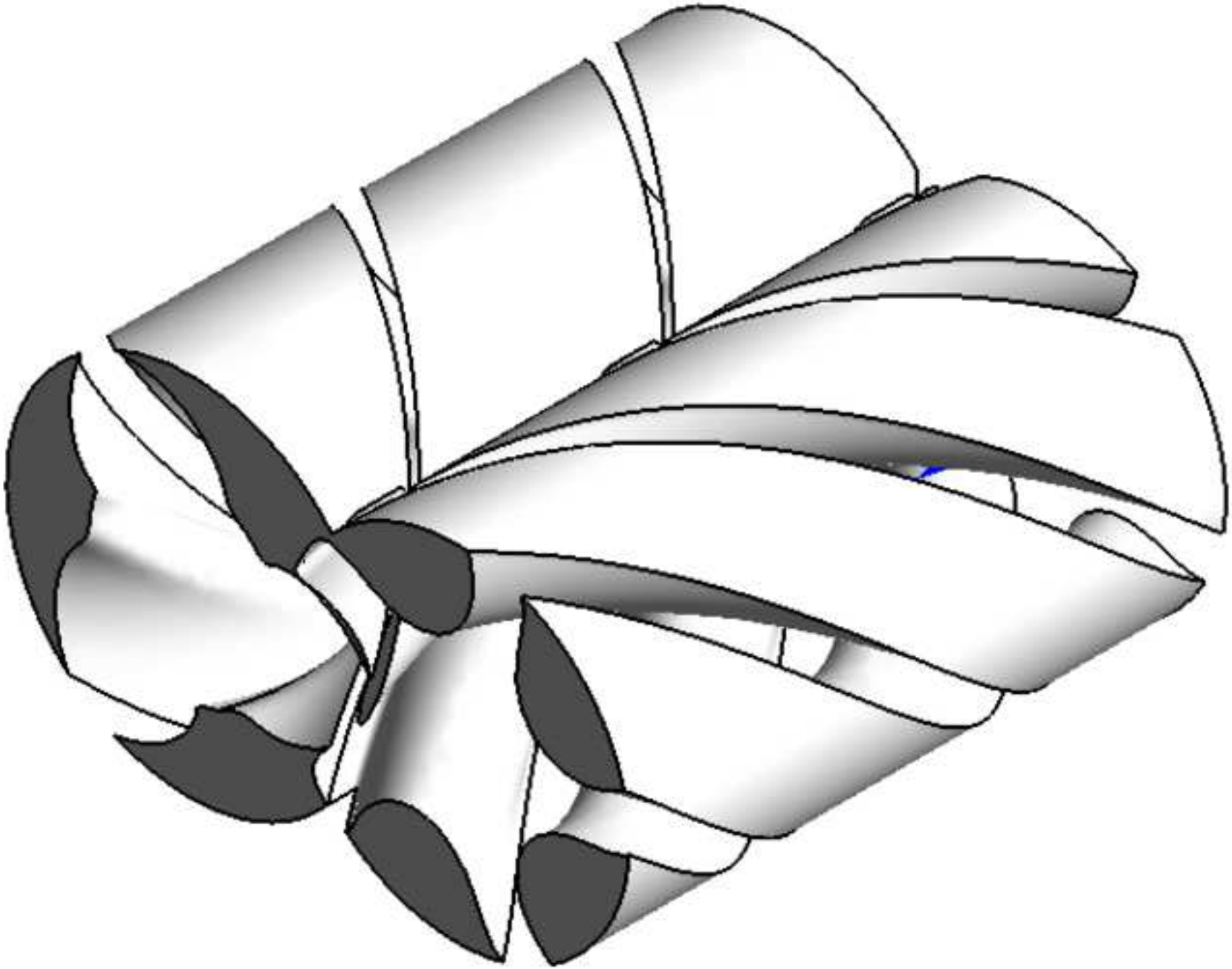

Fig16.tif
Click here to download high resolution image

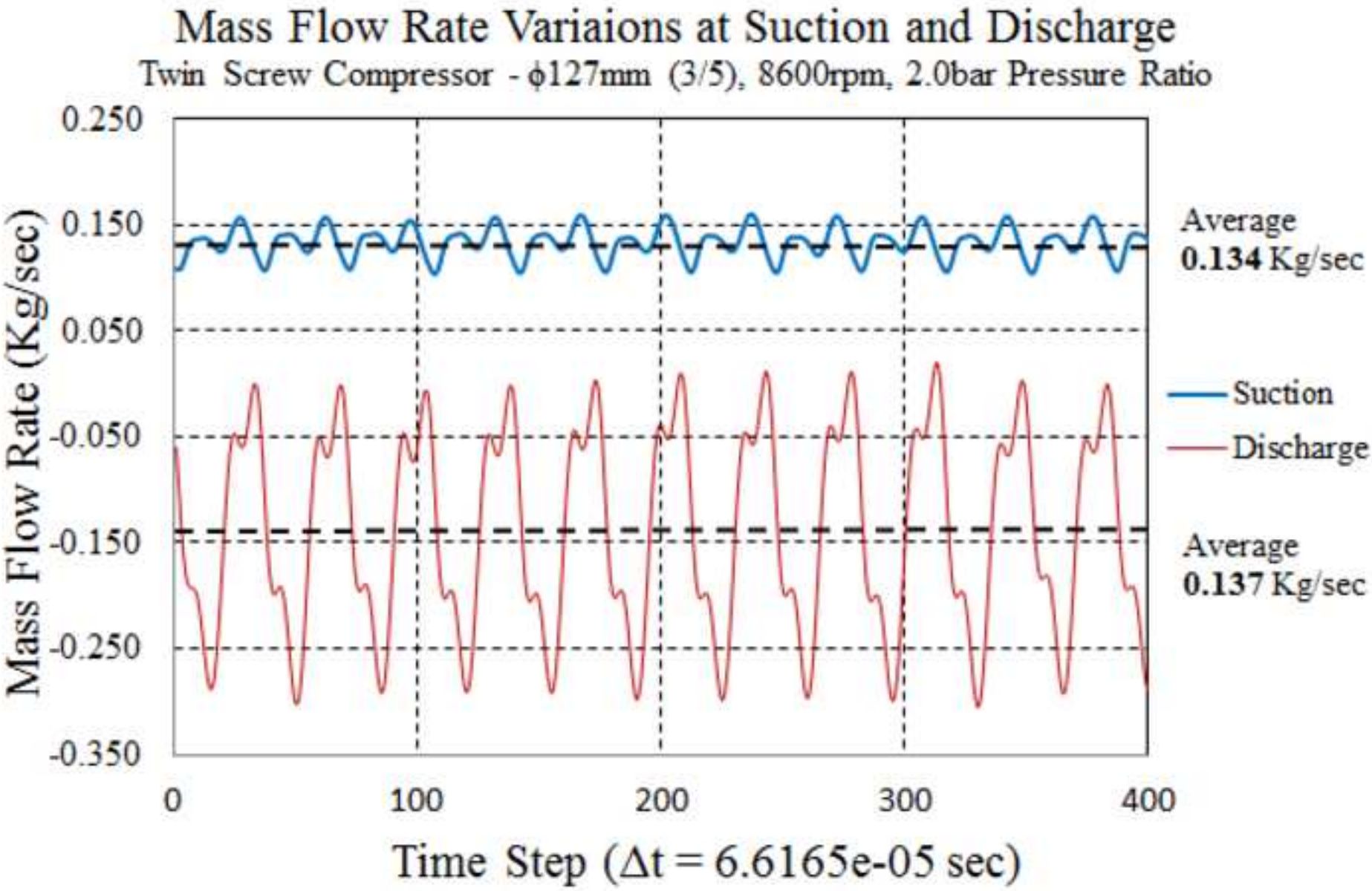

Fig17.tif
Click here to download high resolution image

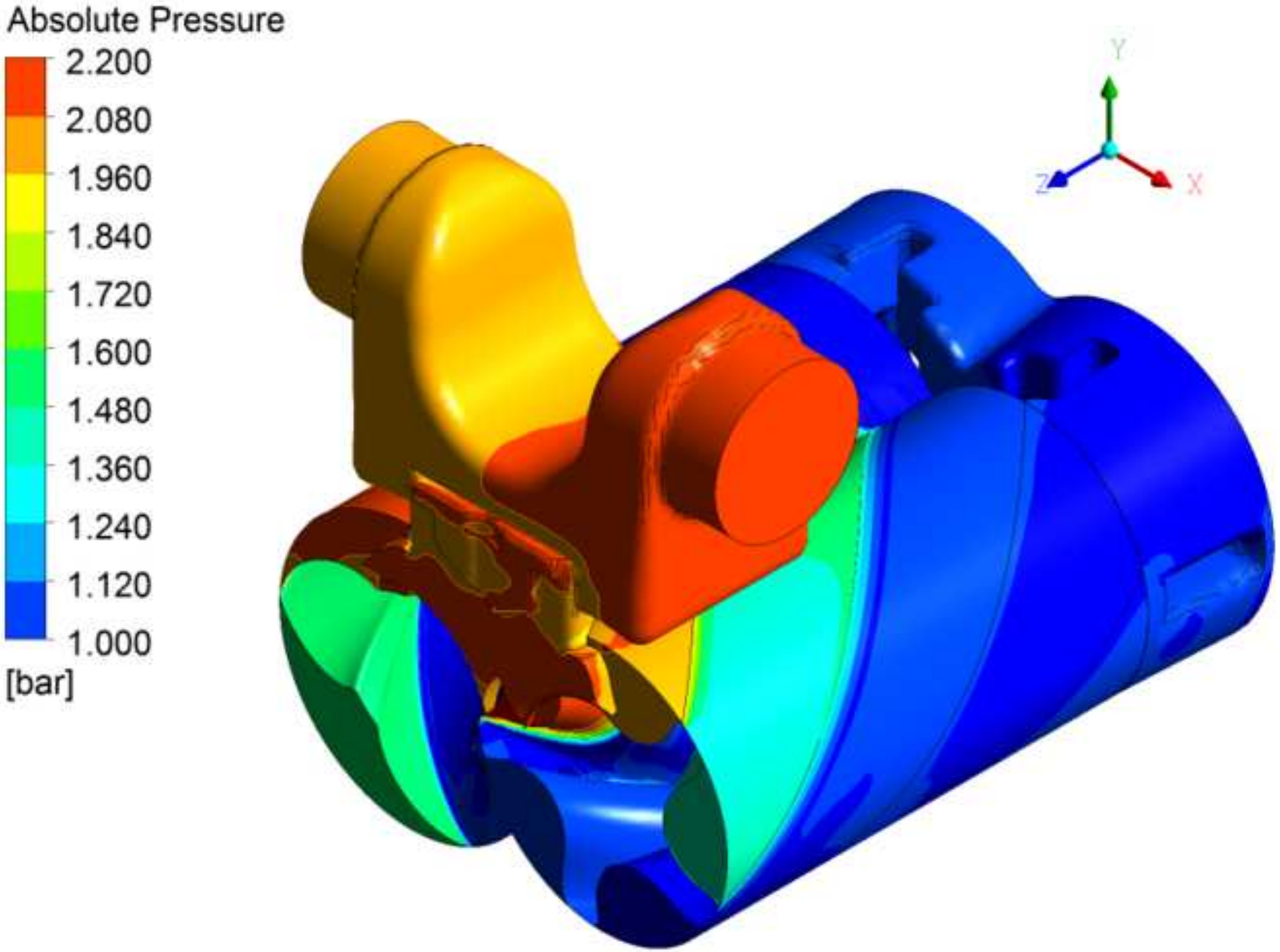

Tables

Table 1 Mesh statistics and errors in results compared to theoretical values

	Cycle	SH1	SH2	SH3	KR1	KR2	KR3	UH1	UH2	UH3
Nubmer of Cells		22752	49962	74720	42098	118749	211418	22752	49962	74720
Number of Nodes		24650	53244	79171	11849	31514	53148	24650	53244	79171
Error in Pressure [%]	**I**	-0.44	-0.44	-0.44	1.17	1.34	1.11	-0.44	-0.44	-0.44
	II	-0.42	-0.42	-0.42	6.23	7.26	7.41	-0.42	-0.42	-0.42
	III	-0.41	-0.41	-0.41	10.55	12.95	14.41	-0.41	-0.41	-0.41
Error in Temperature [%]	**I**	-0.08	-0.08	-0.08	0.05	0.32	0.25	-0.08	-0.08	-0.08
	II	-0.07	-0.07	-0.07	3.44	4.18	3.74	-0.07	-0.07	-0.07
	III	-0.05	-0.05	-0.05	8.56	9.80	10.24	-0.05	-0.05	-0.05
Error in Mass [%]	**I**	-0.38	-0.32	-0.30	1.78	1.91	2.27	-0.38	-0.32	-0.30
	II	-0.38	-0.32	-0.30	2.91	3.21	3.88	-0.38	-0.32	-0.30
	III	-0.38	-0.32	-0.30	2.15	3.29	4.43	-0.38	-0.32	-0.30